Available online at www.sciencedirect.com
SCIENCE DIRECT®
Journal of Organometallic Chemistry 667 (2003) 126–134
Journal of Organometallic Chemistry
www.elsevier.com/locate/jorganchem

Synthesis of Ru(II) complexes of the new 1-[(P-diphenyl)-2-phosphinoethyl]-3,5-dimethylpyrazole ligand and study of their reactivity toward terminal alkynes

Glòria Esquius [a,b], Josefina Pons [a], Ramón Yáñez [a], Josep Ros [a,*], René Mathieu [b,*], Noël Lugan [b], Bruno Donnadieu [b]

[a] Departament de Química, Universitat Autònoma de Barcelona, 08193 Bellaterra-Cerdanyola, Barcelona, Spain
[b] Laboratoire de Chimie de Coordination du CNRS, 250 Route de Narbonne, 31077 Toulouse Cedex 4, France

Received 28 November 2002; received in revised form 5 December 2002; accepted 5 December 2002

Abstract

The reaction between $[RuCl_2(PPh_3)_3]$ and one or two equivalent amounts of 1-[(P-diphenyl)-2-phosphinoethyl]-3,5-dimethylpyrazole (**1**) in dichloromethane gave $[RuCl_2(PPh_3)(\mathbf{1})]$ (**2**) or $[RuCl_2(\mathbf{1})_2]$ (**3**), respectively, in good yields. Activation of propargylic alcohol derivatives by **3** in refluxing dichloromethane and in the presence of $NaBPh_4$ lead to the new allenylidene ruthenium complexes $[RuCl(\mathbf{1})_2(C{=}C{=}CPhCH_3)][BPh_4]$ ([**4**][BPh_4]) and $[RuCl(\mathbf{1})_2(C{=}C{=}CPh_2)][BPh_4]$ ([**5**][BPh_4]). The reaction between **3** and phenylacetylene in dichloromethane and in the presence of KPF_6 affords the vinylidene complex $[RuCl(\mathbf{1})_2(C{=}CHPh)][PF_6]$ ([**6**][PF_6]). The X-ray diffraction studies of **2**, **3**, and [**5**][BPh_4] are reported.

Keywords: Ruthenium; P–N ligands; Hemilabile ligands; Vinylidenes; Allenylidenes

1. Introduction

Transition-metal complexes with polydentate ligands containing both hard and soft donor groups have been extensively used in coordination and organometallic chemistry. The majority of such ligands are functionalized phosphines, where the phosphorus is the soft donor and either oxygen or nitrogen is the hard donor [1,2]. Furthermore, complexes with P–O and P–N ligands have been found to facilitate several stoichiometric transformations of organic molecules, including acetylene to vinylidene tautomerization [3].

The increasing attention brought to the chemistry of ruthenium(II) complexes containing carbene or vinylidene ligands [4–7] is due to their potential ability to promote selective carbon–carbon coupling reactions and to their activity in catalytic transformations involving terminal alkynes [8], ring opening metathesis polymerization (ROMP) or ring closing metathesis (RCM) of cyclic or acyclic olefins [9].

We have recently shown that the new P–N bidentate ligand 1-[(P-diphenyl)-2-phosphinoethyl]-3,5-dimethylpyrazole (**1**) exhibits hemilabile properties when associated to rhodium(I) [10]. So it was tempting to extend our studies of the complexing properties of **1** to the case of ruthenium(II). In this paper we report the synthesis and full characterization—including the X-ray crystal structures—of two new ruthenium(II) complexes containing this ligand, and the study of their reactivity toward phenylacetylene and propargyl alcohols in the direction of vinylidene and allenylidene complexes. The X-ray crystal structure of a new allenylidene–ruthenium is also presented.

2. Results and discussion

1-[(P-diphenyl)-2-phosphinoethyl]-3,5-dimethylpyrazole was synthesized as we described earlier [10] by

* Corresponding authors.
E-mail addresses: josep.ros@uab.es (J. Ros), mathieu@lcc-toulouse.fr (R. Mathieu).

0022-328X/02/$ - see front matter © 2002 Elsevier Science B.V. All rights reserved.
doi:10.1016/S0022-328X(02)02156-3

reaction of 1-(chloroethyl)-3,5-dimethylpyrazole [11] and PPh_2Li in tetrahydrofuran.

The reaction of one equivalent amount of 1-[(P-diphenyl)-2-phosphinoethyl]-3,5-dimethylpyrazole (**1**) with one equivalent amount of $[RuCl_2(PPh_3)_3]$ in dichloromethane at room temperature gave $[RuCl_2(PPh_3)(\mathbf{1})]$ (**2**) in 86% yield (Scheme 1). The complex was analytically and spectroscopically (IR and ^{1}H-, $^{13}C\{^1H\}$-, and $^{31}P\{^1H\}$-NMR) characterized (see Section 4). ^{1}H- and $^{13}C\{^1H\}$-NMR spectra are consistent with the proposed formulation and give evidence for the coordination of the ligand **1** to the Ru(II) atom. Indeed, the $^{31}P\{^1H\}$-NMR spectrum exhibits the expected AX pattern: two doublets at 84.6 and 48.0 ppm ($^2J_{P-P} = 44.0$ Hz) due to the phosphorus atom of the ligand **1** and the one of the triphenylphosphine ligand. The value of the coupling constant is in agreement with two phosphine ligands in a *cis* position [12,13].

The structure of **2** was determined by an X-ray diffraction study. Crystal and refinement data are summarized in Table 1. Selected interatomic distances and angles are provided in Table 2. A perspective view of the complex is shown in Fig. 1.

The ruthenium atom is pentacoordinated through the nitrogen atom N(1) and phosphorus atom P(1) of ligand **1**, the phosphorus atom P(2) of the triphenylphosphine ligand, and two chlorine atoms. The arrangement around the ruthenium atom is intermediate between a square pyramid and a trigonal-bipyramid. Reedijk index of trigonality [14] leads to a square pyramid geometry for the complex with a 19% distortion toward a trigonal bipyramid. In this distorted square pyramid the phosphorus atom P(1) occupies the apical position, while the mean plane containing N(1), P(2), and the two chlorine atoms constitutes the base of the pyramid. The ruthenium atom is 0.327 Å above the base of the pyramid. This allows the N(1)–Ru(1)–P(1) angle to be larger than observed for the same ligand in square-planar rhodium complexes (94.24(6)° as compared with 89.13(7)° for the rhodium complex $[Rh(\mathbf{1})_2]^+$) [10]. Due to the steric bulk of the triphenylphosphine ligand, the P(2)–Ru(1)–Cl(2) and the N(1)–Ru(1)–P(2) angles are greater than 90°—94.09(3) and 92.32(6)°, respectively—and this minimizes the interaction with the methyl group of the pyrazolyl cycle. As a consequence, the N(1)–Ru(1)–Cl(1) and the C(l2)–Ru(1)–Cl(1) angles are lower than 90°, 82.99(6) and 86.92(3)°, respectively. The bond lengths Ru(1)–N(1) (2.105(2) Å), Ru(1)–Cl(1) (2.3979(7) Å) and Ru(1)–Cl(2) (2.3767(7) Å) are in the range of those found in similar complexes [12,15].

The reaction of $[RuCl_2(PPh_3)_3]$ with two equivalent amounts of **1** in dichloromethane solution at room temperature led to $[RuCl_2(\mathbf{1})_2]$ (**3**) in 90% yield (Scheme 1). The analytical and spectroscopic data for this complex are consistent with this formulation. The $^{31}P\{^1H\}$-NMR spectrum shows one signal only at 36.2 ppm for the PPh_2 groups of ligand **1** indicating that the two phosphino groups are magnetically equivalent. The structure of complex **3** was established by an X-ray diffraction analysis. Crystal and refinement data are given in Table 1. Selected bond lengths and angles are provided in Table 2. The complex crystallizes with two independent molecules per unit cell. The two molecules are almost superimposable, the corresponding bond distances and angles being equal within the experimental error. A perspective view of one of the two independent molecules, molecule **A**, is shown in Fig. 2.

The coordination geometry around Ru consists of a distorted octahedron, the two phosphorus atoms and the two nitrogen atoms being respectively in a *cis* position, and the chlorine atoms being in a *trans* position.

The distortion from an idealized octahedral geometry can be attributed to the steric repulsion between of the two bulky PPh_2 and the two close 3,5-dimethylpyrazole groups. The more sterically demanding group is PPh_2 and as a consequence the P(2)–Ru(1)–P(1) angle is the largest (103.73(6)°). The Ru–N distances of 2.216(5) and 2.214(5) Å and the Ru–P bond lengths of 2.2986(16) and 2.3023(16) Å are larger than those found in $[RuCl_2(PPh_3)(\mathbf{1})]$ complex but fall between the experimental values reported for similar complexes [19,22].

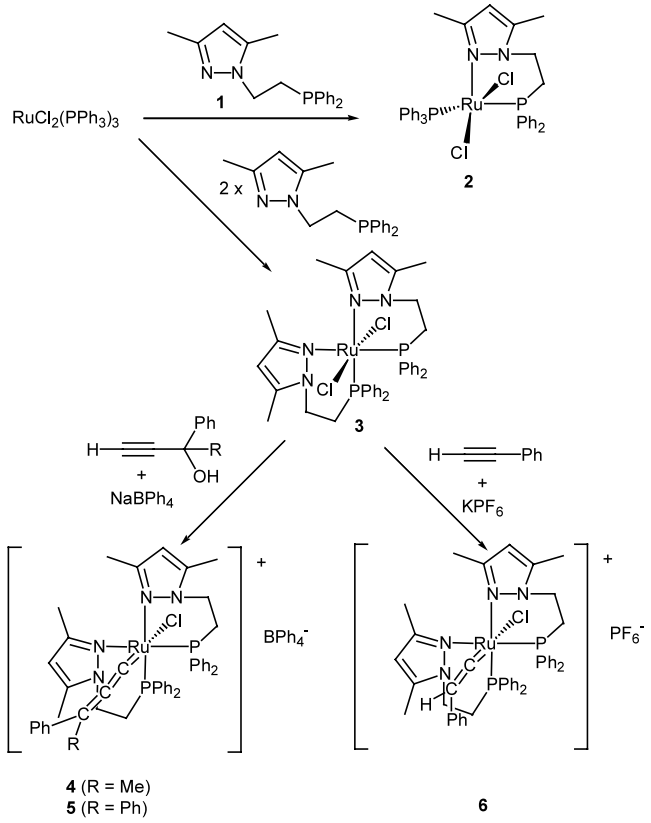

Scheme 1.

Table 1
Crystal data for compounds $[RuCl_2(PPh_3)(\mathbf{1})]$ (**2**), $[RuCl_2(\mathbf{1})_2]$ (**3**), and $[RuCl(\mathbf{1})_2(C{=}C{=}CPh_2)][BPh_4]$ ([**5**][BPh_4])

	2	**3**	[**5**][BPh_4]
Empirical formula	$C_{37}H_{36}Cl_2N_2P_2Ru$	$C_{76}H_{84}Cl_4N_8P_4Ru_2$	$C_{154}H_{144}B_2Cl_2N_8P_4Ru_2$
Formula weight (g)	742.59	1577.33	2525.31
Temperature (K)	293(2)	163(2)	180(2)
Wavelength (Å)	0.71073	0.71073	0.71073
Crystal system	Monoclinic	Monoclinic	Monoclinic
Space group	$P2_1/n$	$P2_1/n$	$P2_1/c$
a (Å)	10.5566(11)	10.9168(9)	23.526(3)
b (Å)	22.1294(18)	43.867(5)	18.6030(14)
c (Å)	14.849(2)	15.5946(12)	30.224(3)
α (°)	90	90	90
β (°)	105.010(14)	106.289(9)	105.869(11)
γ (°)	90	90	90
Volume (Å^3)	3350.6(7)	7168.2(11)	12 724(2)
Z	4	4	4
D_{calc} (g cm^{-3})	1.472	1.462	1.318
μ (mm^{-1})	0.752	0.710	0.387
$F(000)$	1520	3248	5264
θ Range (°)	2.20–25.91	1.95–24.25	1.80–22.60
Index ranges	$-12 \le h \le 12$, $-27 \le k \le 27$, $-18 \le l \le 18$	$-12 \le h \le 12$, $-50 \le k \le 50$, $-17 \le l \le 16$	$-25 \le h \le 25$, $-20 \le k \le 19$, $-32 \le l \le 32$
Reflections collected	24 644	41 978	65 382
Independent reflections	6414 [$R_{int} = 0.0520$]	10 785 [$R_{int} = 0.1136$]	16 562 [$R_{int} = 0.1205$]
Completeness to θ_{max} (%)	98.4	93.0	98.2
Refinement method	Full-matrix least-squares on F^2		
Data/restraints/parameters	6414/0/399	10 785/0/852	16 562/0/1309

The Ru–N distances of 2.216(5) and 2.214(5) Å and the Ru–P bond lengths of 2.299(2) and 2.302(2) Å are larger than those found in complex **2** but fall between the experimental values reported for similar complexes [16,17]. Each of the six-membered rings formed by the bidentate ligands coordinated to ruthenium adopts a boat conformation, the atoms Ru(1) and C(6), and Ru(1) and C(13), respectively, being the apexes of the boats. In addition, in agreement with the NMR data, the apexes are oriented in such a way that the molecule exhibits in the solid state a [non-crystallographic] C_2 symmetry, the C_2 axis passing through the Ru atom and bisecting the P–Ru–P angle. The present structure thus corresponds the ($\lambda\lambda(\delta\delta)$) diastereomers.

The reactivity of the complexes **2** and **3** toward terminal alkynes has been investigated. Reactions of the 16e$^-$ complex **2** with propargylic alcohol or terminal alkynes failed to give any isolatable complexes. Decomposition to metallic ruthenium and free ligands was apparent after prolonged stirring in dichloromethane at room temperature. This is a quite unexpected result as there are precedent for the formation of neutral vinylidene complexes from the 16e$^-$ complexes $RuCl_2(PPh_3)_3$ or $RuCl_2(PPh_3)$(P–N) by reaction with terminal alkynes or propargylic alcohols [18,19].

By contrast, the reaction of the 18e$^-$ complex **3** with 2-phenyl-3-butyn-2-ol or 1,1-diphenyl-2-propyn-1-ol in refluxing dichloromethane and in the presence of $NaBPh_4$ [20,21] afforded the dark red allenylidene–ruthenium complexes, $[RuCl(\mathbf{1})_2(C{=}C{=}CPhCH_3)][BPh_4]$ ([**4**][BPh_4]) and $[RuCl(\mathbf{1})_2(C{=}C{=}CPh_2)][BPh_4]$ ([**5**][BPh_4]) in 82 and 80% yield, respectively (Scheme 1). Both allenylidene complexes were characterized by elemental analysis, IR and NMR spectroscopies. The presence of the allenylidene ligand in complexes [**4**]$^+$ and [**5**]$^+$ was readily established by IR spectroscopy with the observation of strong bands at 1923 and 1936 cm^{-1}, attributable to the $\nu(C{=}C{=}C_{as})$ vibration mode [20]. The NMR spectra of [**4**]$^+$ and [**5**]$^+$ display two different sets of resonances for the two ligands **1**. In particular, ^{1}H-NMR spectra exhibit eight multiplets for the four pairs of diastereotopic protons. On the other hand, the $^{31}P\{^1H\}$-NMR spectra shows two doublets corresponding to the non-equivalent phosphorus atoms. The $^2J_{P-P}$ coupling constant value of 31 Hz (for both complexes) is consistent with the two phosphorus atoms being in a *cis* position. As compared with **3**, these data suggests a lowering of the global symmetry of the complex to the C_1 symmetry. The $^{13}C\{^1H\}$-NMR spectra of complexes [**4**]$^+$ and [**5**]$^+$ display low-field signals at 305.4 ppm (dd, $^2J_{C-P} = 16$ and 19 Hz) and 303.5 (dd, $^2J_{C-P} = 17$ and 19 Hz), respectively, clearly attributable to the C_α of the allenylidene ligands. Resonances due to the C_β carbon atoms and C_γ carbon atoms appear as triplets at 210.8 ppm ($^3J_{C-P} = 3.7$ Hz) and 157.1 ppm ($^4J_{C-P} = 1.8$ Hz), respectively, for [**4**]$^+$,

Table 2
Selected bond distances (Å) and angles (°) for compounds **2**, **3** and **[5]** [BPh_4]

	2		**3**		Cation **5A**	Cation **5B**
Bond lengths						
N(1)–Ru(1)	2.105(2)	N(1)–Ru(1)	2.216(5)	N(1)–Ru(1)	2.171(5)	2.173(5)
P(1)–Ru(1)	2.189(1)	N(3)–Ru(1)	2.214(5)	N(3)–Ru(1)	2.207(5)	2.216(5)
P(2)–Ru(1)	2.270(1)	P(1)–Ru(1)	2.299(2)	P(1)–Ru(1)	2.313(2)	2.333(2)
Cl(1)–Ru(1)	2.398(1)	P(2)–Ru(1)	2.302(2)	P(2)–Ru(1)	2.363(2)	2.356(2)
Cl(2)–Ru(1)	2.377(1)	Cl(1)–Ru(1)	2.431(2)	Cl(1)–Ru(1)	2.448(2)	2.469(2)
		Cl(2)–Ru(1)	2.431(2)	C(15)–Ru(1)	1.878(5)	1.877(6)
				C(15)–C(16)	1.250(8)	1.252(9)
				C(16)–C(17)	1.384(8)	1.364(9)
				C(17)–C(48)	1.464(6)	1.462(7)
				C(17)–C(42)	1.494(6)	1.502(6)
Bond angles						
N(1)–Ru(1)–P(1)	94.24(6)	N(1)–Ru(1)–P(1)	86.32(13)	N(1)–Ru(1)–P(1)	91.27(13)	89.29(14)
N(1)–Ru(1)–P(2)	92.32(6)	N(3)–Ru(1)–P(2)	87.60(14)	N(3)–Ru(1)–P(2)	87.86(14)	85.42(14)
P(1)–Ru(1)–P(2)	95.11(3)	N(1)–Ru(1)–P(2)	167.41(14)	N(1)–Ru(1)–P(2)	164.56(13)	165.31(14)
N(1)–Ru(1)–Cl(1)	82.99(6)	N(3)–Ru(1)–P(1)	167.05(14)	N(3)–Ru(1)–P(1)	172.09(13)	169.10(14)
P(1)–Ru(1)–Cl(1)	108.39(3)	N(3)–Ru(1)–N(1)	83.35(18)	N(1)–Ru(1)–N(3)	86.43(18)	83.04(19)
P(2)–Ru(1)–Cl(1)	156.28(3)	P(1)–Ru(1)–P(2)	103.73(6)	P(1)–Ru(1)–P(2)	96.20(6)	103.30(6)
Cl(2)–Ru(1)–Cl(1)	86.92(3)	N(1)–Ru(1)–Cl(1)	87.21(15)	N(1)–Ru(1)–Cl(1)	85.19(13)	88.45(13)
N(1)–Ru(1)–Cl(2)	167.66(6)	N(3)–Ru(1)–Cl(1)	97.40(15)	N(3)–Ru(1)–Cl(1)	96.29(13)	97.48(13)
P(1)–Ru(1)–Cl(2)	95.67(3)	P(1)–Ru(1)–Cl(1)	89.85(6)	P(1)–Ru(1)–Cl(1)	91.04(5)	90.02(5)
P(2)–Ru(1)–Cl(2)	94.09(3)	P(2)–Ru(1)–Cl(1)	85.29(5)	P(2)–Ru(1)–Cl(1)	81.19(6)	84.06(5)
C(11)–P(1)–C21	99.73(12)	Cl(2)–Ru(1)–Cl(1)	173.22(5)	C(15)–Ru(1)–Cl(1)	178.97(18)	173.40(19)
C(7)–P(1)–C(11)	104.60(12)	N(1)–Ru(1)–Cl(2)	97.89(15)	C(15)–Ru(1)–N(1)	94.9(2)	97.5(2)
C(7)–P(1)–C21	103.58(12)	N(3)–Ru(1)–Cl(2)	87.67(15)	C(15)–Ru(1)–N(3)	84.7(2)	86.1(2)
C(7)–P(1)–Ru(1)	110.45(9)	P(1)–Ru(1)–Cl(2)	86.03(6)	C(15)–Ru(1)–P(1)	87.93(17)	87.19(18)
C(11)–P(1)–Ru(1)	123.03(9)	P(2)–Ru(1)–Cl(2)	90.45(6)	C(15)–Ru(1)–P(2)	98.87(17)	90.76(18)
C(21)–P(1)–Ru(1)	113.33(8)	C(31)–P(1)–Ru(1)	123.4(2)	C(16)–C(15)–Ru(1)	178.0(5)	178.1(5)
C(51)–P(2)–C41	106.46(13)	C(21)–P(1)–Ru(1)	116.7(2)	C(15)–C(16)–C(17)	176.9(6)	176.5(7)
C(51)–P(2)–C(31)	100.21(12)	C(7)–P(1)–Ru(1)	111.1(2)			
C(41)–P(2)–C(31)	99.50(12)	C(41)–P(2)–Ru(1)	123.0(2)			
C(51)–P(2)–Ru(1)	116.04(9)	C(51)–P(2)–Ru(1)	119.7(2)			
C(41)–P(2)–Ru(1)	103.74(9)	C(14)–P(2)–Ru(1)	111.2(2)			
C(31)–P(2)–Ru(1)	128.23(9)					

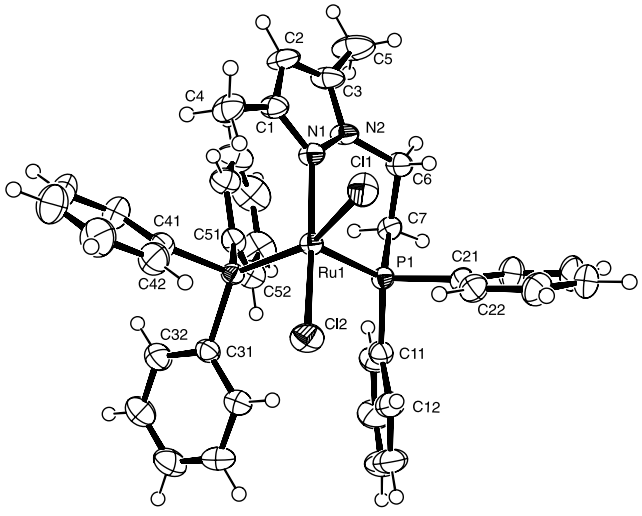

Fig. 1. A perspective view of complex **2** (the thermal ellipsoid are shown at the 50% probability level).

and at 217.9 ppm ($^3J_{C-P} = 3.4$ Hz) and 156.6 ppm ($^4J_{C-P} = 1.8$ Hz), respectively, for $[\mathbf{5}]^+$. These data are comparable to those reported for other allenylidene–ruthenium complexes [21–25].

The molecular structure of complex $[\mathbf{5}]^+$ has been established by X-ray diffraction. Crystal and refinement data are summarized in Table 1. **[5]**[BPh_4] crystallizes with two independent ion pairs per unit cell. Selected interatomic bond distances and angles are provided in Table 2. A perspective view showing one of the two cations, cation **A**, is shown in Fig. 3. The corresponding bond distances within cation **A** and cation **B** are equal within the experimental error. Although most of the corresponding bond angles are significantly different, they remain similar.

Fig. 4 shows a superimposition of the skeleton of the two cations. It appears that the main structural differences lie in the orientation of the phenyl rings attached to P2 ({Ru(1a)–P(2a)–C(30a)–C(31a)} = 7.1°, {Ru(1b)–P(2b)–C(30b)–C(31b)} = −77.1°; {Ru(1a)–P(2a)–C(36a)–C(37a)} = 104.4°, {Ru(1b)–P(2b)–C(36b)–C(37b)} = 13.4°). Each cation consists of a distorted octahedral complex, the angles around Ru

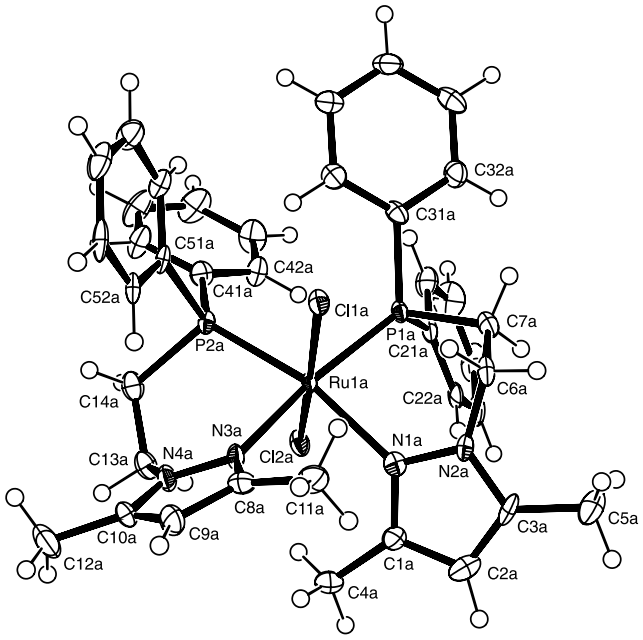

Fig. 2. A perspective view of complex **3** (molecule **A**) (the thermal ellipsoid are shown at the 50% probability level).

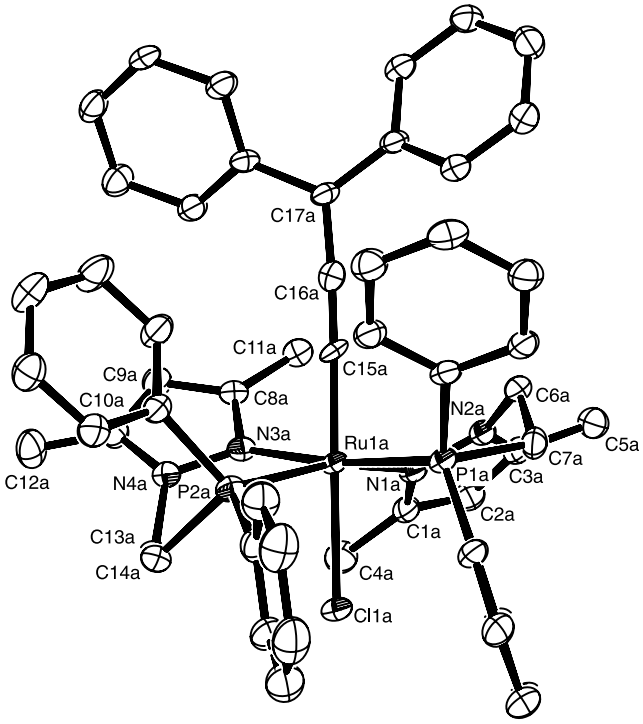

Fig. 3. A perspective view of complex $[5]^+$ (cation **A**) (the thermal ellipsoid are shown at the 30% probability level).

being in the range 81.2–98.9 and 164.6–179.0° for cation **A**, and 83.1–97.5 and 165.3–173.4° for cation **B**. The geometry around the ruthenium atom is similar to that of complex **3**, for which one of the two chlorine atoms would have formally been substituted by the allenylidene ligand. It is worth noting that the $\lambda\lambda(\delta\delta)$

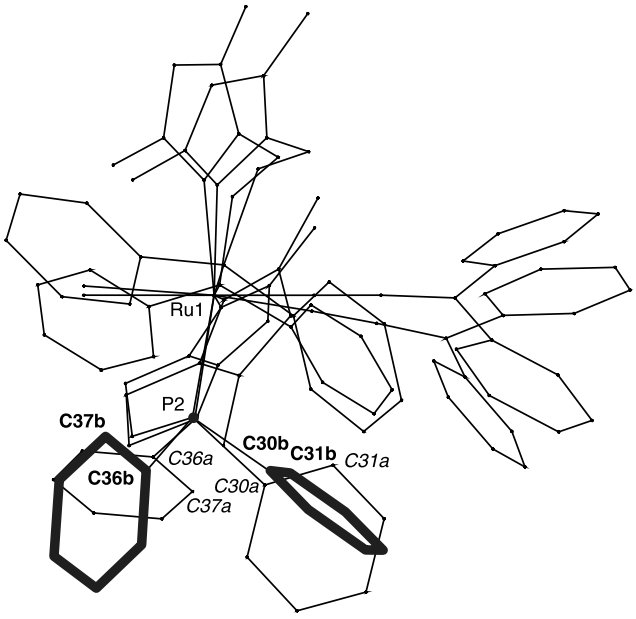

Fig. 4. A superimposition of the skeleton of two independent cations of $[5]^+$, in the solid state.

form is maintained in both cations. The C(15)–Ru–Cl(1) angle is significantly larger for cation **A** (178.97(18)°) than for cation **B** (173.40(19)°). Due to steric crowding around the P atoms, the P–Ru–P angle (96.20(6) and 103.30(6)° for cation **A** and **B**, respectively) is larger than 90°, while the N–Ru–N angle (86.43(18) and 83.04(19)° for cation **A** and **B**, respectively) are smaller than 90°. The diphenylallenylidene ligand is bonded to ruthenium in a nearly linear fashion: Ru(1)–C(15)–C(16) = 178.0(5) and 178.1(5)°, C(15)–C(16)–C(17) = 176.9(6) and 176.5(7)° for cation **A** and **B**, respectively. The bond lengths compare well with those reported for other allenylidene–ruthenium complexes (Ru–C(15) 1.878(5) and 1.877(6) Å, C(15)–C(16) 1.250(8) and 1.252(9) Å, and C(16)–C(17) 1.384(8) and 1.364(9) Å for cations **A** and **B**), respectively [23,24,26,27]. In each cation, the Ru–P and Ru–N bond lengths fall into the expected values for this type of complexes [25,26].

The dynamic properties of complex **5** were assessed a variable-temperature ^{1}H-NMR experiments. No significant change was observed in the 293–320 K range. The solvent and the thermal stability of the complex did not allow acquisition of spectra at higher temperature. Nevertheless, a fluxional behavior was evidenced by phase-sensitive NOESY experiments that indeed clearly showed a dynamic exchange between the corresponding methylene and methyne protons of the two ligands **1**. This observation can be rationalized in terms of a conformational equilibrium between the two six-membered rings allowing the averaging of all isomers of $[5]^+$, $\lambda\lambda(\delta\delta) \leftrightarrows \delta\lambda(\lambda\delta) \leftrightarrows \delta\delta(\lambda\lambda)$.

The reaction of phenylacetylene with complex **3** in dichloromethane at room temperature and in the presence of KPF_6 leads to the vinylidene complex $[RuCl(\mathbf{1})_2(C{=}CHPh)][PF_6]$ ($[\mathbf{6}][PF_6]$), which was isolated as a green solid in 86% yield [16,28]. The salt $[\mathbf{6}][PF_6]$ was characterized by microanalysis, and IR and NMR spectroscopies. Strong infrared absorptions were found at 1623 and 841 cm^{-1} corresponding to the $\nu(C{=}C)$ band of the vinylidene ligand, and to the $[PF_6]^-$ anion, respectively [16,23,28,29]. As for $[\mathbf{5}]^+$, the NMR spectra indicate that the two ligands **1** in $[\mathbf{6}]^+$ are not magnetically equivalent. The most remarkable feature in the ^{1}H-NMR spectrum of $[\mathbf{6}]^+$ is the presence of a triplet signal at 2.97 ppm ($^4J_{P-H} = 4.3$ Hz) attributable to the C=C*H*Ph proton [23,28]. The $^{31}P\{^1H\}$-NMR spectrum exhibits two doublets at 24.4 ppm ($^2J_{P-P} =$ 31.4 Hz) and 22.0 ppm ($^2J_{P-P} = 31.4$ Hz) due to the two non equivalent phosphorus atoms and the small shift difference is consistent with a structure similar to the structure of $[\mathbf{5}]^+$ (Scheme 1). The $^{13}C\{^1H\}$-NMR data clearly indicate the presence of the vinylidene moiety. Significantly, the typical low-field resonance for the C_α carbon atom of the vinylidene moiety appears as a double doublet at 356.8 ppm ($^2J_{C-P} = 16.4$ and 19.2 Hz) while the C_β appears as a singlet at 111.3 ppm. These data are in full agreement, which those reported for other octahedral ruthenium(II) vinylidene derivatives [16,23,28,29].

3. Conclusion

In conclusion, we have shown that the bidentate ligand 1-[(P-diphenyl)-2-phosphinoethyl]-3,5-dimethylpyrazole (**1**) reacts with $[RuCl_2(PPh_3)_3]$ in a straightforward manner to afford either the $16e^-$ complex $[RuCl_2(PPh_3)(\mathbf{1})]$ (**2**) or the $18e^-$ complex $[RuCl_2(\mathbf{1})_2]$ (**3**), depending on the stoichiometry of the reactants. Contrary to our observations in the case of complexation to rhodium [10], no evidences for a hemilabile character of the ligand **1** was obtained when associated to ruthenium in complexes **2** or **3**. On the other hand, in the presence of chloride abstractors, the complex **3** readily activates terminal alkynes to afford in a classical manner cationic cumulene complexes.

4. Experimental

4.1. General

All chemicals were used as received from commercial suppliers, unless otherwise indicated. The complex $RuCl_2(PPh_3)_3$ was prepared according to literature methods [30] and 1-[(P-diphenyl)-2-phosphinoethyl]-3,5-dimethylpyrazole ligand was synthesized as we previously reported [10]. The reactions were carried out under dinitrogen atmosphere using vacuum line and Schlenk techniques. Solvents were dried and distilled according to standard procedures and stored under dinitrogen. NMR spectra were run on Bruker AC200, AC250, Avance DPX250 or Avance DRX500 spectrometers in $CDCl_3$ solutions at room temperature (r.t.). All the chemical shift values are given in ppm and are referenced with respect to residual protons in the solvent for ^{1}H spectra, to solvent signals for ^{13}C spectra, to external H_3PO_4 for ^{31}P spectra and to external C_6H_5F for ^{19}F spectra. IR spectra were recorded on a Perkin–Elmer 2000 spectrophotometer with KBr pellets or in CH_2Cl_2 solutions with CaF_2 cells. Elemental analysis were performed at the Laboratoire de Chimie de Coordination on a Perkin–Elmer 2400 CHN analyzer or at the Universitat Autònoma de Barcelona on a Carlo Erba CHNS EA-1108 apparatus.

4.2. Synthesis of $[RuCl_2(PPh_3)(\mathbf{1})]$ (**2**)

The ligand 1-[(P-diphenyl)-2-phosphinoethyl]-3,5-dimethylpyrazole (**1**) (0.049 g, 0.160 mmol) was added to a solution of 0.153 g (0.160 mmol) of $[RuCl_2(PPh_3)_3]$ in 20 ml of dichloromethane. The green solution was stirred for 5 h. After evaporation of the solvent under vacuum, the addition of 5 ml of acetone gave the compound as a red precipitate, which was filtrated and washed with pentane. The complex was then crystallized in a dichloromethane–acetone mixture. Yield: 86%. Anal. Calc. for $C_{37}H_{36}N_2P_2Cl_2Ru \cdot 1/2CH_2Cl_2$: C, 57.37; H, 4.75; N, 3.57. Found: C, 57.81; H, 4.78; N, 3.43%. IR (KBr) ν (cm^{-1}): 3050 ($\nu C{-}H_{ar}$), 2980–2918 ($\nu C{-}H_{al}$), 1554 ($\nu C{=}C_{ar}$, $\nu C{=}N_{ar}$), 1482–1464 (δCH_{3as}), 1434 ($\delta C{=}C_{ar}$, $\delta C{=}N_{ar}$), 1394–1157 ($\nu C{-}N$), 1090–998 ($\delta C{-}H_{ip}$), 872 ($\delta = CH_{oop}$), 719 ($\nu P{-}C$, $\delta C{-}H_{oop}$). ^{1}H-NMR (200 MHz) δ (ppm): 7.56–7.07 [m, 25H, PPh_2, PPh_3], 5.93 [s, 1H, C*H* pyrazole], 4.17 [m, 2H, $CH_2CH_2PPh_2$], 2.57 [m, 2H, $CH_2CH_2PPh_2$], 2.24 [s, 3H, CCH_3], 2.19 [s, 3H, CCH_3]. $^{13}C\{^1H\}$-NMR (50 MHz) δ (ppm): 148.1 [CCH_3], 140.8 [CCH_3], 140.2–127.3 [PPh_2, PPh_3], 106.9 [*C*H pyrazole], 41.9 [$CH_2CH_2PPh_2$], 31.6 [d, $^1J_{C-P} = 33.6$ Hz, $CH_2CH_2PPh_2$], 15.1 [CCH_3], 11.5 [CCH_3]. $^{31}P\{^1H\}$-NMR (81 MHz) δ (ppm): 84.6 [d, $^2J_{P-P} = 44.0$ Hz, PPh_2], 48.0 [d, $^2J_{P-P} = 44.0$ Hz, PPh_3].

4.3. Synthesis of $[RuCl_2(\mathbf{1})_2]$ (**3**)

The ligand 1-[(P-diphenyl)-2-phosphinoethyl]-3,5-dimethylpyrazole (0.211 g, 0.684 mmol) was added to a solution of 0.306 g (0.320 mmol) of $[RuCl_2(PPh_3)_3]$ in 20 ml of dichloromethane. The brown solution was stirred for 5 h. After evaporation of the solvent under vacuum, the addition of 5 ml of acetone gave the compound as a red precipitate, which was filtrated and washed with pentane. The complex was crystallized in a

dichloromethane–acetone mixture. Yield: 90%. Anal. Calc. for $C_{38}H_{42}Cl_2N_4P_2Ru$: C, 57.87; H, 5.37; N, 7.10. Found: C, 57.14; H, 4.65; N, 6.73%. IR (KBr) ν (cm^{-1}): 3054 ($\nu C–H_{ar}$), 2964–2919 ($\nu C–H_{al}$), 1554 ($\nu C=C_{ar}$, $\nu C=N_{ar}$), 1480 (δCH_{3as}), 1435 ($\delta C=C_{ar}$, $\delta C=N_{ar}$), 1371–1154 ($\nu C–N$), 1096–1030 ($\delta C–H_{ip}$), 717 ($\nu P–C$, $\delta C–H_{oop}$). ^{1}H-NMR (250 MHz) δ (ppm): 7.26–7.02 [m, 20H, PPh_2], 5.84 [s, 2H, C*H* pyrazole], 5.17 [m, 4H, $CH_2CH_2PPh_2$], 2.72 [m, 4H, $CH_2CH_2PPh_2$], 2.27 [s, 6H, CCH_3], 1.99 [s, 6H, CCH_3]. $^{13}C\{^1H\}$-NMR (63 MHz) δ (ppm): 155.0 [CCH_3], 140.3 [CCH_3], 134.3–126.9 [PPh_2], 108.4 [*C*H pyrazole], 43.8 [$CH_2CH_2PPh_2$], 33.5 [d, $^1J_{C-P} = 25.7$ Hz, $CH_2CH_2PPh_2$], 15.5 [CCH_3], 12.0 [CCH_3]. $^{31}P\{^1H\}$-NMR (101 MHz) δ (ppm): 36.2 [b, PPh_2].

4.4. Synthesis of [RuCl(1)$_2$(C=C=CPhCH$_3$)][BPh$_4$] [4][BPh$_4$]

2-Phenyl-3-butyn-2-ol in dichloromethane (0.034 g, 0.231 mmol)) and 0.032 g (0.093 mmol) of $NaBPh_4$ in the minimum of methanol were added to a solution of 0.073 g (0.093 mmol) of $[RuCl_2(\mathbf{1})_2]$ in 10 ml of dichloromethane. The mixture was heated under reflux for 1 h. The solvents were evaporated under reduced pressure. The residue was dissolved in 10 ml of dichloromethane and the salts were separated by filtration. After evaporation, the remaining red solid was washed with diethyl ether and dried under vacuum. The complex was crystallized in a dichloromethane–diethyl ether. Yield: 82%. Anal. Calc. for $C_{72}H_{70}BClN_4P_2Ru$: C, 72.03; H, 5.88; N, 4.67. Found: C, 71.94; H, 6.13; N, 4.70%. IR (KBr) ν (cm^{-1}): 3050–3034 ($\nu C–H_{ar}$), 2994–2922 ($\nu C–H_{al}$), 1936 ($\nu C=C=C_{as}$), 1557 ($\nu C=C_{ar}$, $\nu C=N_{ar}$), 1479 (δCH_{3as}), 1434 ($\delta C=C_{ar}$, $\delta C=N_{ar}$), 1370–1161 ($\nu C–N$), 1095–1030 ($\delta C–H_{ip}$), 721 ($\nu B–C$, $\nu P–C$, $\delta C–H_{oop}$). ^{1}H-NMR (250 MHz) δ (ppm): 7.38–6.79 [m, 45H, PPh_2, C*Ph*CH_3, BPh_4], 6.39 [m, 1H, C*H*HCH_2PPh_2], 5.90 [s, 1H, C*H* pyrazole], 5.87 [s, 1H, C*H* pyrazole], 4.53 [m, 1H, C*H*HCH_2PPh_2], 4.43 [m, 1H, CH*H*CH_2PPh_2], 4.02 [m, 1H, CH*H*CH_2PPh_2], 2.90 [m, 1H, CH_2CHPPh_2], 2.74 [m, 1H, CH_2CHPPh_2], 2.70 [m, 1H, CH_2CHPPh_2], 2.31 [s, 3H, CCH_3], 2.12 [m, 1H, CH_2CHPPh_2], 2.07 [s, 3H, CCH_3], 2.01 [s, 3H, CCH_3], 1.31 [s, 3H, CCH_3], 1.26 [s, 3H, $CPhCH_3$]. $^{13}C\{^1H\}$-NMR (63 MHz) δ (ppm): 305.4 [dd, $^2J_{C-P} = 16.5$ and 19.6 Hz, Ru=*C*], 210.8 [t, $^3J_{C-P} = 3.7$ Hz, Ru=C=*C*], 164.3 [q, $^1J_{C-11B} = 49.4$ Hz, BPh_4], 164.3 [sept, $^1J_{C-10B} = 16.6$ Hz, BPh_4], 157.1 [t, $^4J_{C-P} = 1.8$ Hz, Ru=C=C=*C*], 155.7 [d, $^3J_{C-P} = 2.5$ Hz, CCH_3], 154.2 [CCH_3], 142.9 [CCH_3], 142.5 [d, $^4J_{C-P} = 1.8$ Hz, CCH_3], 136.4–121.7 [PPh_2, C*Ph*CH_3, BPh_4], 109.5 [d, $^4J_{C-P} = 2.5$ Hz, *C*H pyrazole], 108.8 [d, $^4J_{C-P} = 1.8$ Hz, *C*H pyrazole], 43.8 [$CH_2CH_2PPh_2$], 32.5 [d, $^1J_{C-P} = 33.1$ Hz, $CH_2CH_2PPh_2$], 31.5 [d, $^1J_{C-P} = 33.1$ Hz, $CH_2CH_2PPh_2$], 15.7 [CCH_3], 15.4 [$CPhCH_3$], 14.0 [CCH_3], 12.2 [$2 \times CCH_3$]. $^{31}P\{^1H\}$-NMR (101 MHz) δ (ppm): 30.2 [d, $^2J_{P-P} = 31.4$ Hz, PPh_2], 28.1 [d, $^2J_{P-P} = 31.4$ Hz, PPh_2].

4.5. Synthesis of [RuCl(1)$_2$(C=C=CPh$_2$)][BPh$_4$] [5][BPh$_4$]

1,1-Diphenyl-2-propyn-1-ol (0.046 g, 0.222 mmol) in dichloromethane and 0.030 g (0.089 mmol) of $NaBPh_4$ dissolved in the minimum of methanol were added to a solution of 0.070 g (0.089 mmol) of $[RuCl_2(\mathbf{1})_2]$ in 10 ml of dichloromethane. The mixture was heated under reflux for 1 h. After cooling at r.t., the solvents were removed under vacuum. The residue was extracted with dichloromethane and the salts were separated by filtration. The red solution was then evaporated under vacuum and the remaining complex was crystallized in dichloromethane–diethyl ether. Yield: 80%. Anal. Calc. for $C_{77}H_{72}BClN_4P_2Ru$: C, 73.24; H, 5.75; N, 4.44. Found: C, 73.07; H, 5.87; N, 4.42%. IR (KBr) ν (cm^{-1}): 3051 ($\nu C–H_{ar}$), 2996–2931 ($\nu C–H_{al}$), 1923 ($\nu C=C=C_{as}$), 1558 ($\nu C=C_{ar}$, $\nu C=N_{ar}$), 1480 (δCH_{3as}), 1433 ($\delta C=C_{ar}$, $\delta C=N_{ar}$), 1374–1129 ($\nu C–N$), 1093–1030 ($\delta C–H_{ip}$), 720 ($\nu B–C$, $\nu P–C$, $\delta C–H_{oop}$). ^{1}H-NMR (250 MHz) δ (ppm): 7.41–6.82 [m, 50H, PPh_2, CPh_2, BPh_4], 6.36 [m, 1H, C*H*HCH_2PPh_2], 5.89 [s, 2H, C*H* pyrazole], 4.79 [m, 1H, C*H*HCH_2PPh_2], 4.34 [m, 1H, CH*H*CH_2PPh_2], 4.07 [m, 1H, CH*H*CH_2PPh_2], 2.90 [m, 1H, CH_2CHPPh_2], 2.66 [m, 1H, CH_2CHPPh_2], 2.61 [m, 1H, CH_2CHPPh_2], 2.27 [s, 3H, CCH_3], 2.14 [m, 1H, CH_2CHPPh_2], 2.06 [s, 3H, CCH_3], 2.02 [s, 3H, CCH_3], 1.37 [s, 3H, CCH_3]. $^{13}C\{^1H\}$-NMR (63 MHz) δ (ppm): 303.5 [dd, $^2J_{C-P} = 17.5$ and 19.3 Hz, Ru=*C*], 217.9 [t, $^3J_{C-P} = 3.4$ Hz, Ru=C=*C*], 164.3 [q, $^1J_{C-11B} = 49.4$ Hz, BPh_4], 164.3 [sept, $^1J_{C-10B} = 16.6$ Hz, BPh_4], 156.6 [t, $^4J_{C-P} = 1.8$ Hz, Ru=C=C=*C*], 155.6 [d, $^3J_{C-P} = 2.5$ Hz, CCH_3], 154.1 [CCH_3], 144.8 [CCH_3], 142.8 [d, $^4J_{C-P} = 1.8$ Hz, CCH_3], 136.3–121.6 [PPh_2, CPh_2, BPh_4], 109.6 [d, $^4J_{C-P} = 2.5$ Hz, *C*H pyrazole], 108.8 [d, $^4J_{C-P} = 1.8$ Hz, *C*H pyrazole], 43.9 [d, $^2J_{C-P} = 28.8$ Hz, $2 \times CH_2CH_2PPh_2$], 33.0 [d, $^1J_{C-P} = 31.9$ Hz, $CH_2CH_2PPh_2$], 32.2 [d, $^1J_{C-P} = 31.9$ Hz, $CH_2CH_2PPh_2$], 15.7 [CCH_3], 14.3 [CCH_3], 12.1 [$2 \times CCH_3$]. $^{31}P\{^1H\}$-NMR (101 MHz) δ (ppm): 31.2 [d, $^2J_{P-P} = 31.4$ Hz, PPh_2], 26.6 [d, $^2J_{P-P} = 31.4$ Hz, PPh_2].

4.6. Synthesis of [RuCl(1)$_2$(C=CHPh)][PF$_6$] [6][PF$_6$]

Phenylacetylene (19.5 μl, 0.178 mmol) and 0.033 g (0.178 mmol) of potassium hexafluorophosphate were added to a solution of 0.070 g (0.089 mmol) of $[RuCl_2(\mathbf{1})_2]$ in 25 ml of dichloromethane. After 4 h under stirring, the salts were separated off by filtration and the solution was evaporated under vacuum. The green residue was washed with diethyl ether and dried in

vacuo. Yield: 86%. Anal. Calc. for $C_{46}H_{48}ClF_6N_4P_3Ru \cdot O(CH_2CH_3)_2$: C, 55.89; H, 5.44; N, 5.21. Found: C, 55.94; H, 5.84; N, 4.94%. IR (KBr) ν (cm^{-1}): 3054 (νC–H_{ar}), 2978–2924 (νC–H_{al}), 1623 (νC=C), 1559 (νC=C_{ar}, νC=N_{ar}), 1487 (δCH_{3as}), 1434 (δC=C_{ar}, δC=N_{ar}), 1378–1159 (νC–N), 1096–1039 (δC–H_{ip}), 841 (νP–F), 720 (νP–C, δC–H_{oop}). ^{1}H-NMR (250 MHz) δ (ppm): 7.43–6.78 [m, 25H, PPh_2, CH*Ph*], 6.35 [m, 1H, C*H*HCH_2PPh_2], 5.96 [s, 1H, C*H* pyrazole], 5.92 [s, 1H, C*H* pyrazole], 5.74 [m, 1H, C*H*HCH_2PPh_2], 4.76 [m, 1H, CH*H*CH_2PPh_2], 4.57 [m, 1H, CH*H*CH_2PPh_2], 3.06 [m, 1H, CH_2C*H*HPPh_2], 2.97 [t, $^4J_{H-H} = 4.3$ Hz, 1H, Ru=C=C*H*Ph], 2.84 [m, 1H, CH_2C*H*HPPh_2], 2.80 [m, 1H, CH_2CH*H*PPh_2], 2.44 [s, 3H, CC*H*$_3$], 2.36 [s, 3H, CC*H*$_3$], 2.25 [m, 1H, CH_2CH*H*PPh_2], 2.00 [s, 3H, CC*H*$_3$], 1.45 [s, 3H, CC*H*$_3$]. ^{13}C{^{1}H}-NMR (63 MHz) δ (ppm): 356.8 [dd, $^2J_{C-P} = 16.4$ and 19.2 Hz, Ru=*C*], 156.9 [d, $^3J_{C-P} = 2.1$ Hz, *C*CH_3], 154.6 [*C*CH_3], 144.6 [*C*CH_3], 144.1 [*C*CH_3], 134.7–126.2 [PPh_2, CH*Ph*], 111.3 [Ru=C=*C*HPh], 110.0 [*C*H pyrazole], 108.9 [*C*H pyrazole], 43.8 [d, $^2J_{C-P} = 34.1$ Hz $2 \times C$$H_2CH_2PPh_2$], 32.2 [d, $^1J_{C-P} = 32.7$ Hz, CH_2*C*H_2PPh_2], 29.9 [d, $^1J_{C-P} = 33.4$ Hz, CH_2*C*H_2PPh_2], 15.4 [C*C*H_3], 15.3 [C*C*H_3], 12.1 [$2 \times$C*C*H_3]. ^{31}P{^{1}H}-NMR (101 MHz) δ (ppm): 24.4 [d, $^2J_{P-P} = 31.4$ Hz, PPh_2], 22.0 [d, $^2J_{P-P} = 31.4$ Hz, PPh_2], −143.4 [sept, $^1J_{P-F} = 711.7$ Hz, PF_6]. ^{19}F{^{1}H}-NMR (235 MHz) δ (ppm): −73.6 [d, $^1J_{F-P} = 711.7$ Hz, PF_6].

4.7. X-ray crystallographic study

Crystals of complexes **2**, **3**, and [**5**][BPh_4] suitable for X-ray diffraction were obtained through recrystallization from dichloromethane–ether mixtures. Data were collected on a STOE IPDS diffractometer at r.t. for **2**, at 163 K for **3**, and at 180 K for [**5**][BPh_4]. Full crystallographic data for the three complexes are gathered in Table 1. All calculations were performed on a PC-compatible computer using the WINGX system [31]. The structures were solved by using the SIR92 program [32], which revealed in each instance the position of most of the non-hydrogen atoms. All remaining non-hydrogen atoms were located by the usual combination of full-matrix least-squares refinement and difference electron density syntheses by using the SHELXS97 program [33]. Atomic scattering factors were taken from the usual tabulations [34]. Anomalous dispersion terms for Ru, P and Cl atoms were included in F_c [35]. All non-hydrogen atoms were allowed to vibrate anisotropically. All the hydrogen atoms were set in idealized position (R_3CH, C–H = 0.96 Å; R_2CH_2, C–H = 0.97 Å; C(sp^2)–H = 0.93 Å; U_{iso} 1.2 time greater than the U_{eq} of the carbon atom to which the hydrogen atom is attached) and held fixed during refinements.

5. Supplementary material

The crystallographic CIF files have been deposited with the Cambridge Crystallographic Data Centre (deposition numbers: CCDC 195652 (**2**), CCDC 195653 (**3**), CCDC 195654 ([**5**][BPh_4]). Copies of this information may be obtained free of charge from: The Director, CCDC, 12 Union Road, Cambridge, CB2 1EZ, UK (Fax: +44-1223-336033; e-mail: deposit@ccdc.cam.ac.uk or www: http://www.ccdc.cam.ac.uk).

Acknowledgements

Support by the CNRS and the Ministerio de Educación y Cultura of Spain (Projects PB96-1146 and BQU200-0238 and grant to G.E.) are gratefully acknowledged.

References

[1] A. Bader, E. Lindner, Coord. Chem. Rev. 108 (1991) 27.
[2] C.S. Slone, D.A. Weinberger, C.A. Mirkin, Prog. Inorg. Chem. 48 (1999) 233.
[3] See for instance: (a) H. Werner, M. Schulz, B. Windmüller, Organometallics 14 (1995) 3659; (b) E. Lindner, M. Geprägs, K. Gierling, R. Fawzi, M. Steimann, Inorg. Chem. 34 (1995) 6106; (c) J.Y. Shen, C. Slugovc, P. Wiede, K. Mereiter, R. Schmid, K. Kirchner, Inorg. Chim. Acta 268 (1998) 69; (d) C. Slugovc, P. Wiede, K. Mereiter, R. Schmid, K. Kirchner, Organometallics 16 (1997) 2768.
[4] V. Cadierno, J. Diez, M.P. Gamasa, J. Gimeno, E. Lastra, Coord. Chem. Rev. 193–195 (1999) 147.
[5] M.I. Bruce, Chem. Rev. 98 (1998) 2797.
[6] M.C. Puerta, P. Valerga, Coord. Chem. Rev. 193–195 (1999) 977.
[7] D. Touchard, P.H. Dixneuf, Coord. Chem. Rev. 178–180 (1998) 409.
[8] C. Bruneau, P.H. Dixneuf, Acc. Chem. Res. 32 (1999) 311.
[9] T.M. Trnka, R.H. Grubbs, Acc. Chem. Res. 34 (2001) 18.
[10] G. Esquius, J. Pons, R. Yáñez, J. Ros, R. Mathieu, B. Donnadieu, N. Lugan, Eur. J. Inorg. Chem. (2002) 2999.
[11] P. Cabildo, R.M. Claramunt, P. Cornago, J.L. Lavandera, D. Sanz, N. Jagerovic, M.L. Jimeno, J. Elguero, I. Gilles, J.L. Aubagnac, J. Chem. Soc. Perkin Trans. (1996) 701.
[12] Y. Arikawa, M. Ueoka, K. Matoba, Y. Nishibayashi, M. Hidai, S. Uemura, J. Organomet. Chem. 572 (1999) 163.
[13] C.R.S.M. Hampton, I.R. Butler, W.R. Cullen, B.R. James, J.P. Charland, J. Simpson, Inorg. Chem. 31 (1992) 5509.
[14] A.W. Addison, T. Nageswara Rao, J. Reedijk, J. Van Rijn, G.C. Verschoor, J. Chem. Soc. Dalton Trans. (1984) 1349.
[15] Y. Nishibayashi, I. Takei, S. Uemura, M. Hidai, Organometallics 17 (1998) 3420.
[16] J.Y. Shen, C. Slugovc, P. Wiede, K. Mereiter, R. Schmid, K. Kirchner, Inorg. Chim. Acta 268 (1998) 69.
[17] H. Yang, N. Lugan, R. Mathieu, C. R. Acad. Sci. IIC2 4 (1999) 251.
[18] Y. Wakatsuki, H. Yamazaki, N. Kumegawa, T. Satoh, J.Y. Satoh, J. Am. Chem. Soc. 113 (1991) 9604.
[19] R. Mathieu, unpublished results.
[20] J.P. Selegue, Organometallics 1 (1982) 217.

[21] D. Touchard, N. Pirio, P.H. Dixneuf, Organometallics 14 (1995) 4920.
[22] V. Cadierno, S. Conejero, M.P. Gamasa, J. Gimeno, M.A. Rodríguez, Organometallics 21 (2002) 203.
[23] B. Buriez, I.D. Burns, A.F. Hill, A.J.P. White, D.J. Williams, J.D.E.T. Wilton-Ely, Organometallics 18 (1999) 1504.
[24] I. de los Ríos, M. Jiménez Tenorio, M.C. Puerta, P. Valerga, J. Organomet. Chem. 549 (1997) 221.
[25] V. Cadierno, M.P. Gamasa, J. Gimeno, L. Iglesias, Inorg. Chem. 38 (1999) 2874.
[26] M.C.B. Colbert, J. Lewis, N.J. Long, P.R. Raithby, M. Younus, A.J.P. White, D.J. Williams, N.N. Payne, L. Yellowless, D. Beljonne, N. Chawdhury, R.H. Friend, Organometallics 17 (1998) 3034.
[27] D. Touchard, N. Pirio, L. Toupet, M. Fettouhi, L. Ouahab, P.H. Dixneuf, Organometallics 14 (1995) 5263.
[28] D. Touchard, P. Haquette, N. Pirio, L. Toupet, P.H. Dixneuf, Organometallics 12 (1993) 3132.
[29] M.A. Jiménez Tenorio, M. Jiménez Tenorio, M.C. Puerta, P. Valerga, Organometallics 19 (2000) 1333.
[30] P.S. Hallman, T.A. Stephenson, G. Wilkinson, Inorg. Synth. 12 (1970) 237.
[31] L.J. Farrugia, J. Appl. Crystallogr. 32 (1999) 837.
[32] A. Altomare, G. Cascarano, C. Giacovazzo, A. Guagliardi, J. Appl. Crystallogr. 26 (1993) 343.
[33] G.M. Sheldrick, SHELXS97, SHELXL97, CIFTAB—Programs for Crystal Structure Analysis (Release 97-2), Institüt für Anorganische Chemie der Universität, Tammanstrasse 4, D-3400 Göttingen, Germany, 1998.
[34] (a) D.T. Cromer, J.T. Waber, International Tables for X-ray Crystallography, vol. 4 (Table 22B), Kynoch Press, Birmingham, England, 1974;
(b) R.F. Stewart, E.R. Davidson, W.T. Simpson, J. Chem. Phys. 42 (1965) 3175;
(c) T. Hahn (Ed.), International Tables for Crystallography, vol. A, Kluwer Academic Publishers, Dordrecht, The Netherlands, 1995.
[35] D.T. Cromer, J.T. Waber, International Tables for X-ray Crystallography, vol. 4 (Table 2.3.1), Kynoch Press, Birmingham, UK, 1975.